Reconstituted Syntaxin1A/SNAP25 Interacts with Negatively Charged Lipids as Measured by Lateral Diffusion in Planar Supported Bilayers

Michael L. Wagner and Lukas K. Tamm
Department of Molecular Physiology and Biological Physics and Center for Structural Biology, University of Virginia Health Sciences Center, Charlottesville, Virginia 22908 USA

ABSTRACT According to the soluble *N*-ethylmaleimide-sensitive factor (NSF)-attachment protein (SNAP) receptor hypothesis (SNARE hypothesis), interactions between target SNAREs and vesicle SNAREs (t- and v-SNAREs) are required for membrane fusion in intracellular vesicle transport and exocytosis. The precise role of the SNAREs in tethering, docking, and fusion is still disputed. Biophysical measurements of SNARE interactions in planar supported membranes could potentially resolve some of the key questions regarding the mechanism of SNARE-mediated membrane fusion. As a first step toward this goal, recombinant syntaxin1A/SNAP25 (t-SNARE) was reconstituted into polymer-supported planar lipid bilayers. Reconstituted t-SNAREs in supported bilayers bound soluble green fluorescent protein/vesicle-associated membrane protein (v-SNARE), and the SNARE complexes could be specifically dissociated by NSF/α-SNAP in the presence of ATP. The physiological activities of SNARE complex formation were thus well reproduced in this reconstituted planar model membrane system. A large fraction ($\sim$75%) of the reconstituted t-SNARE was laterally mobile with a lateral diffusion coefficient of 7.5×10^{-9} cm^2/s in a phosphatidylcholine lipid background. Negatively charged lipids reduced the mobile fraction of the t-SNARE and the lipids themselves. Phosphatidylinositol-4,5-bisphosphate was more effective than phosphatidylserine in reducing the lateral mobility of the complexes. A model of how acidic lipid-SNARE interactions might alter lipid fluidity is discussed.

INTRODUCTION

SNARE molecules are central players in membrane fusion in exocytosis and intracellular vesicle transport (Südhof et al., 1989; Bennett et al., 1992; Söllner et al., 1993b; Hayashi et al., 1994; Rothman and Wieland, 1996; Hanson et al., 1997; Ungermann et al., 1998; Chao et al., 1999; Jahn and Südhof, 1999; Brünger, 2000). The SNARE complex, which forms at some stage before, during, or after fusion, consists of SNAREs of target membranes (t-SNAREs) and SNAREs of the secretory vesicle membranes (v-SNAREs). The neuronal SNARE complex forms from the t-SNARE complex consisting of syntaxin1A and SNAP-25 and the v-SNARE synaptobrevin. When combined in solution, the t- and v-SNAREs form a coiled-coil structure of four parallel α-helices (Sutton et al., 1998; Poirier et al., 1998). It has been suggested that this SNARE complex constitutes the minimal protein machinery sufficient to mediate fusion of two lipid bilayers (Weber et al., 1998; Parlati et al., 1999). There is also evidence that after (or before) each round of fusion, NSF (Block et al., 1988) in conjunction with α-SNAP (Clary et al., 1990) dissociates the SNARE complex in a reaction that requires ATP (Söllner et al., 1993a; Hayashi et al., 1995). Various other accessory and regulatory proteins control the dynamics of t- and v-SNARE association and are thus important at some stage of exocytosis. Synaptotagmin is the Ca^{2+} sensor in synaptic membrane fusion (Brose et al., 1992; Sutton et al., 1999). nSec1 binds to syntaxin1A, and its release from that complex is required to form the four-helix SNARE complex (Misura et al., 2000). Rab (small G) proteins are effectors of membrane fusion, possibly by interaction with nSec1 (Ferro-Novick and Novick, 1993; Ostermeier and Brünger, 1999). Despite an enormous amount of accumulated knowledge on these proteins, which in many cases includes the determination of their structures, the precise sequence of events and which proteins exactly are responsible for tethering, docking, fusion, and recycling of the SNAREs is not yet known. One possible approach to sort out the respective roles of the individual proteins is to reconstitute the fusion process from purified components. A first step in this direction has been taken by

Received for publication 14 December 2000 and in final form 2 April 2001.

Address reprint requests to Dr. Lukas Tamm, Department of Molecular Physiology and Biological Physics and Center for Structural Biology, University of Virginia Health Sciences Center, P.O. Box 800736, Charlottesville, VA 22908-0736. Tel.: 434-982-3578; Fax: 434-982-1616; E-mail: lkt2e@virginia.edu.

Abbreviations used: BoNT, botulinum neurotoxin; DPS, 1,2-dimyristoyl-*sn*-glycero-3-phosphoethanolamine-PEG3400-triethoxysilane; DOPS, 1,2-dioleoyl-*sn*-glycero-3-[phospho-L-serine]; DOPC, 1,2-dioleoyl-*sn*-glycero-3-phosphocholine; FRAP, fluorescence recovery after photobleaching; GFP, green fluorescent protein; NBD-eggPE, *N*-(7-nitrobenz-2-oxa-1,3-diazol-4-yl)-egg phosphatidylethanolamine, NBD-PIP_2, 1-[6-[(7-nitrobenz-2-oxa-1,3-diazol-4-yl) amino]hexanoyl]-2-hexanoyl-*sn*-glycero-phosphoinositol-4,5-bisphosphate, NBD-PS, 1-palmitoyl-2-[12-[(7-nitrobenz-2–1,3-benzoxadiazol-4-yl) amino] dodecanoyl]-*sn*-glycero-3-phosphoserine; NEM, *N*-ethylmaleimide; NSF, *N*-ethylmaleimide-sensitive factor; β-OG, β-octylglucoside; PEG, poly(ethylene glycol); PIP_2, phosphatidylinositol-4,5-bisphosphate; POPC, 1-palmitoyl-2-oleoyl-*sn*-glycero-3-phosphocholine; RB, reconstitution buffer (25 mM HEPES/KOH, 100 mM KCl, pH 7.4); SPB, supported planar bilayer; SNAP, soluble NSF-attachment protein; SNAP-25, synaptosome-associated protein of 25 kDa; SNARE, SNAP receptor; t-SNARE, target SNARE; TIRFM, total internal reflection fluorescence microscopy; v-SNARE, vesicle SNARE; VAMP, vesicle-associated membrane protein; VAMPh, hydrolytic VAMP.

© 2001 by the Biophysical Society

0006-3495/01/07/266/10 $2.00

Rothman and co-workers who showed that fusion, albeit slow, is supported by t- and v-SNAREs alone (Weber et al., 1998; Parlati et al., 1999).

Reconstitution procedures in solution are somewhat limited to address some of the most pertinent questions because tethering, docking, and fusion are not easily separated in these assays. Simple rate constants determined from in vitro fusion experiments contain only limited information about all the interactions that are taking place during this complicated process. Here, we propose to study the relevant interactions between SNARE (and potentially other) molecules in a planar membrane system on solid supports by evanescent wave microscopy or TIRFM. This method is ideally suited to quantitatively measure the binding of soluble or vesicular ligands to membrane receptors (Kalb et al., 1990). Fusion can be studied in this system in combination with FRAP measurements (Hinterdorfer et al., 1994) or by monitoring the release of fluorescent tracer molecules by TIRFM (Zenisek et al., 2000; Toomre et al., 2000). In this approach, the receptors of interest are reconstituted into planar lipid bilayers that are supported on quartz microscope slides. Supported membranes have been widely used in the past as models for cellular membranes (for reviews see McConnell et al., 1986; Sackmann, 1996). Supported lipid bilayers on solid supports exhibit fully mobile lipids in both leaflets of the bilayer (Tamm, 1988). Until recently, a concern for the reconstitution of integral membrane proteins into supported lipid bilayers was the small (~10 Å) separation between the bilayer and the solid support. This space was not sufficient to accommodate hydrophilic protein domains on the inner side of the bilayer, and interactions of these domains with the hydrophilic solid support inhibited the lateral mobility of receptor proteins in the lipid bilayer. To alleviate some of these problems, we recently devised a strategy to support lipid bilayers on a tethered polymer cushion of PEG that was inserted between the bilayer and the solid support (Wagner and Tamm, 2000). This strategy allowed us to reconstitute several integral membrane proteins into supported lipid bilayers in a laterally mobile form. Dynamic membrane processes that require the lateral rearrangement of participating integral membrane proteins can now be studied in these tethered polymer-supported bilayers. Here, we show that t-SNAREs can be functionally reconstituted in supported lipid bilayers in a form that maintains their normal lateral mobility. We use TIRFM and FRAP to study their interactions with v-SNAREs and with membrane lipids. Specifically, we show that reconstituted syntaxin1A/SNAP-25 in supported bilayers reversibly binds VAMP and that the negatively charged lipids phosphatidylserine and, more effectively, phosphatidylinositol-4,5-bisphosphate decrease the lateral mobility of the reconstituted t-SNAREs in a concentration-dependent manner.

MATERIALS AND METHODS

Materials

Expressed syntaxin1A/SNAP25-His_6 (Parlati et al., 1999), GFP-VAMP, VAMPh (McNew et al., 1999), which lacks the transmembrane domain, His_6-NSF-myc (Söllner et al., 1993a), his_6-α-SNAP (Whiteheart et al., 1994), and his_6-BoNT D light chain (Glenn and Burgoyne, 1996) were kind gifts of Dr. James Rothman (Memorial Sloan-Kettering Cancer Center). POPC, DOPS, NBD-PS, PIP_2 from swine brain, and NBD-eggPE were from Avanti Polar Lipids (Alabaster, AL). NBD-PIP_2 was from Echelon Research Laboratories (Salt Lake City, UT). Alexa Fluor 488 succinimidyl ester and rabbit anti-Alexa 488 antibody were from Molecular Probes (Eugene, OR). β-OG, creatine phosphate, creatine kinase (rabbit muscle), NEM, and ATP were from Sigma (St. Louis, MO). Quartz slides (37 mm × 25 mm × 1 mm) were from Quartz Scientific (Fairport Harbor, OH). DPS (Wagner and Tamm, 2000) was custom-synthesized by Shearwater Polymers (Huntsville, AL).

Total internal reflection fluorescence microscopy

The TIRFM apparatus, mounted on a vibration-controlled table, was built around a Zeiss Axiovert 35 microscope. Fluorescence from an integrated sample area was detected with a photometric accessory and an EMI 9658A photomultiplier tube. Fluorescence images were recorded on another port with an EG&G 512 × 512 cooled charge-coupled device camera (PARC, Princeton, NJ). A specially cut trapezoid quartz prism was mounted to a Peltier element on the condenser holder and optically coupled with glycerol to the top of a quartz slide, which formed the roof of the sample cell. The Peltier element was used to regulate the temperature of the sample cell. The home-built perfusable sample cell (Tamm, 1993) had inner dimensions of 22 × 30 × 1 mm^3. The beam of an Innova 300–8W argon ion laser (Coherent, Palo Alto, CA) was directed through an AOM-40 acousto-optic modulator (IntraAction, Bellwood, IL) and a focusing lens into the prism and sample at an angle of 72° from the normal. The greater than critical angle of incidence ensured total internal reflection at the lower surface of the quartz slide and the creation of an evanescent wave at the ceiling of the sample cell. The 1/e penetration depth of the evanescent wave under these conditions is 90 nm. The acousto-optic modulator was used to regulate the beam intensity. A standard 488/515-nm dichroic mirror and emission filter were used. Fluorescence was collected from the bottom of the cell through a 40× (0.75 numerical aperture) water immersion objective. Mechanical shutters (Vincent Associates, Rochester, NY) were placed in the excitation and emission paths to protect sample and photomultiplier tube from overexposure. The laser intensity and mechanical shutters were controlled and data were collected with a personal computer and an automated program using Labview (National Instruments, Austin, TX) software.

Fluorescent labeling and reconstitution of t-SNAREs into liposomes

Syntaxin1A/SNAP-25 (t-SNARE) was stored in small aliquots in 25 mM HEPES/KOH containing 100 mM KCl, 10% glycerol, 1 mM dithiothreitol and 1% β-OG at −80°C. t-SNAREs were fluorescently labeled by thawing an aliquot and reacting the complex with Alexa Fluor 488 succinimidyl ester after adjusting the pH to 8.3 with 1 M sodium bicarbonate. Unreacted label was removed on a Sephadex G-25 spin column equilibrated with 1% β-OG in RB (25 mM HEPES/KOH, 100 mM KCl, pH 7.4). The resulting Alexa/protein ratio was 1:3 (mol:mol) as determined by absorbance spectroscopy (ϵ_{494}(Alexa 488) = 71,000 M^{-1} cm^{-1}) and the Biorad protein assay. Alexa-488-labeled t-SNAREs stored at 4°C were used within 1 week. To reconstitute t-SNAREs into proteoliposomes, lipids were mixed from chloroform stock solutions, dried under N_2, and placed under vacuum for 30 min. Fluorescent lipid probes were included at this step if desired.

The dried lipid films were fully solubilized with a volume of 1% β-OG in RB followed by the addition of a volume of syntaxin1A/SNAP-25 to give a final volume of 100 μl and the desired protein:lipid ratio. The mixture was equilibrated at room temperature for 1 h followed by addition of 200 μl of RB to bring the β-OG concentration below the critical micellar concentration. The mixture was dialyzed for 19 h against 1 L of RB at 4°C with one change of buffer. The lipid:protein ratio of the resulting t-SNARE vesicles was determined by the Biorad protein assay and a modified Ames phosphate assay (Ames, 1966) to estimate lipid concentrations.

Reconstitution of t-SNAREs into polymer-supported bilayers

Planar bilayers supported on a thethered 3 mol % DPS PEG cushion were prepared as previously described (Wagner and Tamm, 2000). To incorporate t-SNAREs into polymer-supported bilayers, monolayers consisting of 97 mol % DOPC and 3 mol % DPS were transferred at 32 mN/m onto quartz slides by the Langmuir-Blodgett technique. Single supported bilayers were then formed by a self-assembly process after flowing 1.1 ml of reconstituted t-SNARE vesicles (100 μM lipid) into the TIRFM measuring cell. Lipid vesicles (with or without protein) are known to spread on (or fuse with) the hydrophobic surface of the supported monolayer under these conditions (Kalb et al., 1992). This method produces a single bilayer composed of a Langmuir-Blodgett-derived inner monolayer and a proteoliposome-derived outer monolayer (Fig. 1). The kinetics of bilayer formation were followed by TIRFM (Kalb et al., 1990). After 2 h of equilibration at room temperature, excess unfused t-SNARE vesicles were flushed out of the cell with 5 vol of RB. The t-SNARE-containing lipid bilayers were then treated by flushing the cell with 5 vol of RB adjusted to pH 5.0, followed by a 20-min equilibration before returning the pH to 7.4 by flushing with RB. This pH treatment heals relatively rare defects in supported lipid bilayers (Tamm and McConnell, 1985; Cremer and Boxer, 1999) and was found here to improve the lateral diffusion measurements in the PEG-supported bilayers.

SNARE complex formation and dissociation

Soluble GFP-VAMP (200 μg/ml) was added to supported t-SNARE bilayers in RB, and the binding was followed by TIRFM as described above. The experiments were carried out at room temperature or at 37°C as indicated. The higher temperature was maintained with a Peltier element that was built into the quartz prism holder. After the fluorescence intensity had reached a constant value, nonspecifically bound GFP-VAMP was washed away with 10 ml of RB. To measure the dissociation of SNARE complexes in supported bilayers, they were first treated with 2 ml of a solution containing 0.12 μM NSF, 1.4 μM α-SNAP, 0.7 μM VAMPh, 100 μg/ml creatine kinase, 100 mM creatine phosphate, 1 mM ATP, and 1 mM EDTA. After 5–10 min of equilibration, 2 ml of the dissociation solution, which contained 0.12 μM NSF, 1.4 μM α-SNAP, 0.7 μM VAMPh, 100 μg/ml creatine kinase, 100 mM creatine phosphate, 1 mM ATP, and 3 mM $MgCl_2$, was added. An excess of nonfluorescent VAMPh was included in this solution to replace dissociated GFP-VAMP. The fluorescence changes were monitored by TIRFM. After dissociation was complete, the bilayer was washed with 5 ml of RB. In some control experiments, 140 μg of his_6-BoNT D light chain in 2 ml of RB was added at the end of the dissociation reaction. No fluorescence was released from the membrane surface in these experiments.

Lateral diffusion measurements

Lateral diffusion of proteins and lipids in supported bilayers was measured by FRAP as described in detail elsewhere (Tamm, 1988; Kalb et al., 1992; Wagner and Tamm, 2000). The same laser fluorescence microscope was used as for the TIRFM experiments, except that the laser beam was expanded and directed into the epi-illumination path. In these experiments, a pattern of parallel stripes with a periodicity of 12.7 μm was imaged onto an ~150-μm diameter area of the sample. The integrated fluorescence from this area was measured as a function of time and stored in the

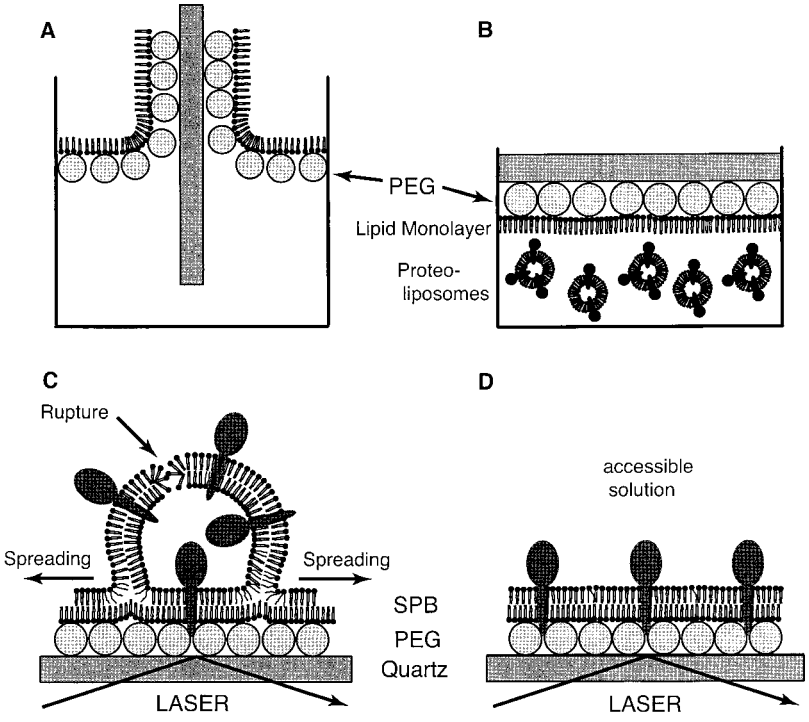

FIGURE 1 Preparation of polymer-supported bilayers with incorporated t-SNAREs. (*A*) A polymer-lipid monolayer is transferred onto a quartz slide by the Langmuir-Blodgett technique. (*B*) Proteoliposomes containing t-SNAREs are injected into the chamber under a polymer-supported lipid monolayer. (*C*) Proteoliposomes spread spontaneously on the polymer-supported monolayer. We think that the vesicle that is under tension during spreading ruptures at some point to complete the spreading process. (*D*) A polymer-supported bilayer with reconstituted t-SNAREs after excess proteoliposomes have been flushed out of the measuring cell. The figures in *C* and *D* are inverted relative to their actual orientation on the microscope.

computer. The fluorescence recovery curves recorded after an ~100-ms bleach pulse were fit to the equation:

$$F(t) = F_\infty + (F_0 - F_\infty)\exp(-D_L\, a^2 t), \quad (1)$$

where D_L is the lateral diffusion coefficient, $a = 2\pi$/(stripe period), and F_0 and F_∞ are the fluorescence intensities immediately after and a very long time after the bleach pulse, respectively. In pattern photobleaching, the mobile fraction in percent is defined as

$$MF = [(F - F_0)/(F_{pre} - F_0)] \times 200, \quad (2)$$

where F_{pre} is the fluorescence intensity before the bleach pulse.

RESULTS AND DISCUSSION

Reconstituted t-SNAREs are laterally mobile in polymer-supported bilayers

We prepared planar lipid bilayers containing t-SNAREs on a polymer support as depicted in Fig. 1. We showed previously that our combined Langmuir-Blodgett/self-assembly method leads to single planar lipid bilayers that are continuous, relatively defect free at the level of resolution of a light microscope, and fluid with respect to lipid diffusion in both leaflets of the lipid bilayer (Wagner and Tamm, 2000). In our earlier work, we also demonstrated that two membrane proteins, cytochrome b_5 and annexin V, were relatively free to diffuse laterally in polymer-supported bilayers, but not in bilayers that were directly supported on quartz microscope slides. The polymer, a 3400-Da PEG, was chosen because it shows minimal interactions with proteins, lipids, and quartz and because it behaves like a nearly ideal random polymer in aqueous buffers. To stabilize the supported bilayers, we covalently tethered the linear polymer to the quartz support at one end and to 3 mol % of the lipids in the bilayer at the other end. To visualize the incorporation of t-SNAREs into supported bilayers, the proteins were labeled with Alexa 488 at a ratio of 1–3 fluorophores per 60-kD complex. Alexa 488 was chosen as a fluorophore because its fluorescence is high and insensitive to pH changes and because it is more photostable than fluorescein. The top right panel of Fig. 2 shows an epifluorescence micrograph of a reconstituted planar bilayer of POPC on a tethered PEG3400 support containing t-SNAREs that were reconstituted at a molar ratio of 400:1 lipid:protein. At first sight, the fluorescence appears quite uniform over the entire viewing area, indicating a continuous single bilayer membrane with no visible defects. Upon closer inspection, some speckling is observed, which indicates that the distribution of the t-SNAREs in the plane of the membrane is not completely homogeneous. Some, but not all, t-SNAREs may aggregate into clusters at this lipid:protein ratio (see below). When in a similarly prepared 400:1 POPC:t-SNARE bilayer the lipid moiety was labeled with 2 mol % NBD-eggPE, the fluorescence distribution was completely uniform at the resolution of the light microscope (Fig. 2, top left panel). Therefore, the lipids appear homogeneously distributed in this preparation. Because we used a NA = 0.75 objective, inhomogeneities (or defects) larger than ~300 nm [$(\lambda/(2 \times \mathrm{NA})$] would have been observed if they were present.

Syntaxin1A contains a single transmembrane domain at its very C-terminus. SNAP-25 forms a coiled-coil complex with the cytoplasmic domain of syntaxin1A. SNAP-25 has no transmembrane sequence, but it binds to membranes via several Cys-linked palmitoyl chains. To demonstrate that most t-SNAREs were reconstituted with their cytoplasmic domains facing outwards, i.e., away from the polymer and quartz slide, we used a fluorescence-quenching anti-Alexa 488 antibody. In 1% β-OG buffer solution, this antibody quenched up to 87% of the fluorescence of Alexa-488-labeled t-SNAREs (at a fivefold excess of antibody:t-SNARE by weight; data not shown). When 80 μg/ml of this antibody was added to Alexa-labeled t-SNAREs in polymer-supported bilayers they quenched 74% of the initial fluorescence (Fig. 3). Therefore, we conclude that at least 85% of the t-SNAREs were reconstituted right side out as depicted in Fig. 1 *D*.

We next measured lateral diffusion of the t-SNAREs in the polymer-supported bilayer by FRAP (filled circles in Fig. 4). These FRAP curves obtained at a lipid:protein ratio of 500:1 in a DOPC:DPS (97:3)/POPC bilayer could be fitted to a single exponential (Eq. 1), indicating a single mobile component. The lateral diffusion coefficient averaged from this and several other curves that were obtained under identical conditions was $7.5 \pm 1.0 \times 10^{-9}$ cm^2/s, and the mobile fraction (Eq. 2) was 78 ± 3% (Table 1). For comparison, the fluorescent lipid analog NBD-eggPE included in the outer monolayer diffused at $6.0 \pm 1.5 \times 10^{-9}$ cm^2/s with a mobile fraction of 79 ± 2% (open squares in Fig. 4; Table 1). Table 1 lists more lateral diffusion data of NBD-eggPE and Alexa-t-SNARE under different conditions. Decreasing the protein concentration to 1000:1 lipid:protein leaves the lateral diffusion coefficient of NBD-eggPE unchanged at $6.5 \pm 0.5 \times 10^{-9}$ cm^2/s and increases its mobile fraction slightly to 88 ± 2%. The lateral diffusion coefficient of the t-SNAREs decreased slightly to $5.0 \pm 1.0 \times 10^{-9}$ cm^2/s, and the mobile fraction decreased to 44 ± 7% when the protein concentration was increased to 400:1 lipid:protein. This smaller fraction may be related to the more speckled appearance of these bilayers in Fig. 2 and the formation of some t-SNARE clusters under these conditions. When the bilayers were supported directly on quartz, slightly larger diffusion coefficients and mobile fractions were observed for the lipids and proteins at all protein concentrations (Table 1). Somewhat surprisingly and in contrast to cytochrome b_5 or annexin V (Wagner and Tamm, 2000), the t-SNAREs were mobile in these bilayers as well. A plausible explanation for this observation is that syntaxin1A ends with the hydrophobic transmembrane domain at its C-terminus (Bennett et al., 1992). However, although the t-SNAREs diffuse freely in quartz-supported

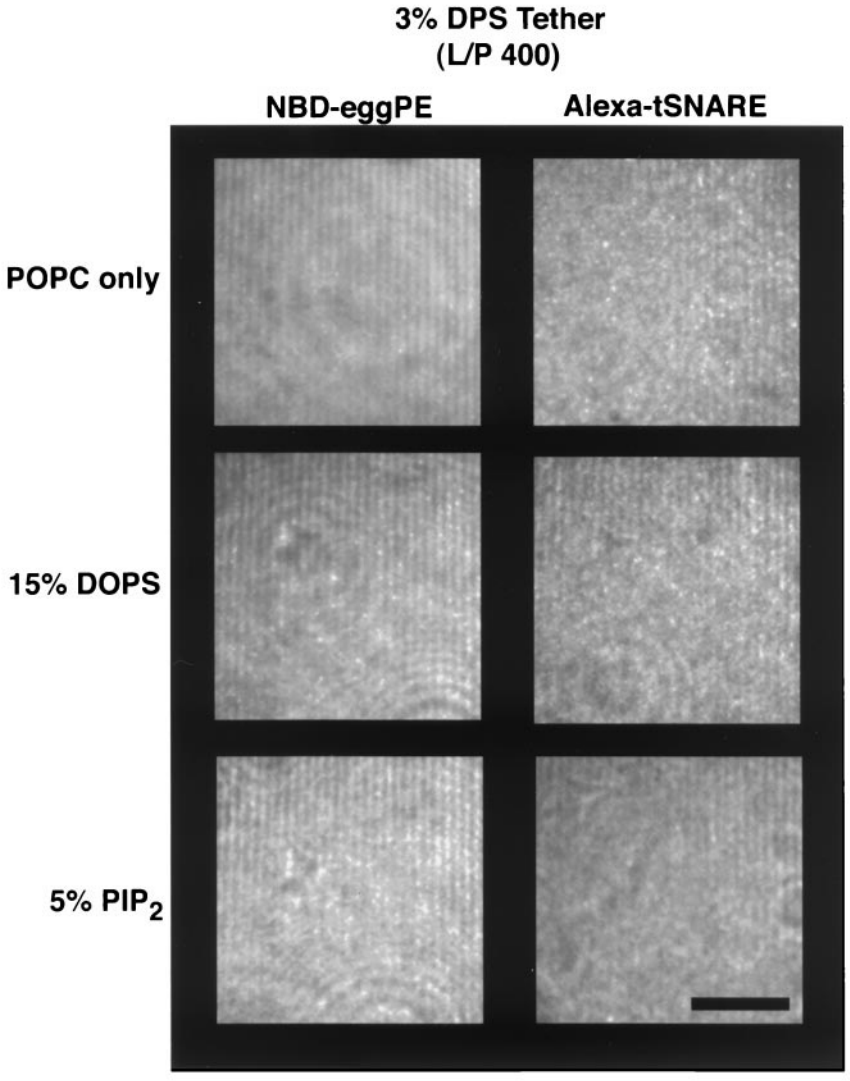

FIGURE 2 Epifluorescence micrographs of t-SNAREs in a PEG-supported bilayer. All bilayers were composed of DOPC:DPS (97:3) in the bottom leaflet and POPC and, where indicated, 15 mol % DOPS or 5 mol % PIP_2 in the top leaflet. They all contained syntaxin 1A/SNAP-25 at a lipid:protein ratio of 400:1. The bilayers were labeled with 2 mol % of the lipid probe NBD-eggPE (*left column*) or Alexa 488 that was bound to the t-SNAREs. The bar is 25 μm.

bilayers, we believe that bilayers that are supported on soft polymer cushions are more plastic and perhaps better physiological membrane models than bilayers on hard supports, especially for future studies of membrane fusion in this system. Therefore, most of our subsequent experiments were carried out with the PEG-supported bilayers.

Reconstituted t-SNAREs bind soluble v-SNAREs

We wanted to know whether the reconstituted t-SNAREs (syntaxin1A/SNAP-25) were able to bind the cognate v-SNAREs (VAMP) in our model system. This was tested with a GFP-labeled soluble VAMP construct. In this fusion protein the GFP was fused to the N-terminus, i.e., the membrane-distal end of VAMP. We again used TIRFM to follow the binding of soluble GFP-VAMP to PEG-supported and quartz-supported t-SNARE bilayers. GFP-VAMP bound rapidly and up to high levels to reconstituted t-SNARE bilayers that were formed from POPC and t-SNAREs at a lipid:protein ratio of 400:1 (Fig. 5). However, some of this protein was bound nonspecifically. About 45% of the GFP-VAMP was removed when the bilayer was washed with RB, but approximately 55% appears to be specifically bound to the t-SNARE bilayer (Fig. 5).

SNARE complexes in supported bilayers are dissociated by NSF/α-SNAP

NSF and α-SNAP are known to dissociate SNARE complexes in a reaction that requires ATP. To prove that the remaining GFP-VAMP was bound in a specific complex with the t-SNAREs, we treated the reconstituted complexes with NSF/α-SNAP in the presence and absence of ATP. In the experiment of Fig. 5, a solution containing NSF, α-SNAP, VAMPh, creatine kinase, creatine phosphate, ATP, and EDTA was added at 43 min. NSF requires Mg-

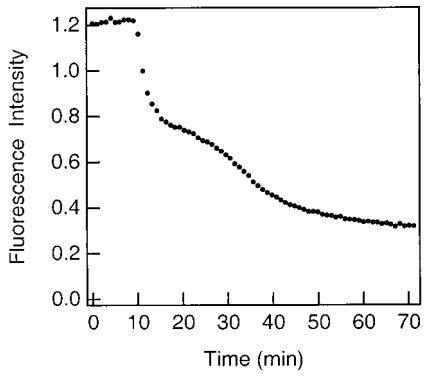

FIGURE 3 Binding of an anti-Alexa-488 antibody to Alexa-488-labeled t-SNAREs in a PEG-supported bilayer consisting of POPC at a lipid: protein ratio of 400:1. The quenching of the Alexa 488 fluorescence is measured by TIRFM at room temperature. The extent of quenching (74%) shows that most fluorophores are accessible to the antibody and therefore that most t-SNAREs (85%) are oriented right side out, i.e., with their cytoplasmic domains as shown in Fig. 1 *D*.

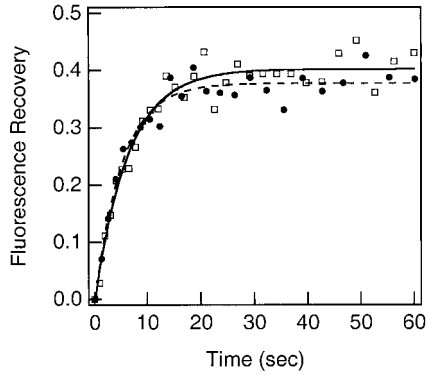

FIGURE 4 Lateral diffusion of lipid and t-SNARE in a PEG-supported bilayer. Unlabeled or Alexa-488-labeled syntaxin1A/SNAP25 were reconstituted into supported bilayers at a lipid:protein ratio of 500:1. □, Fluorescence recovery of 2 mol % NBD-eggPE in the outer monolayer of supported bilayers consisting of DOPC:DPS (97:3)/POPC containing unlabeled syntaxin1A/SNAP25. The diffusion coefficient and mobile fraction derived from a single exponential fit (——) were 6.5×10^{-9} cm^2/s and 82%, respectively. ●, Fluorescence recovery of Alexa-labeled syntaxin1A/SNAP25 reconstituted into a supported bilayer consisting of DOPC:DPS(97:3)/POPC. The diffusion coefficient and mobile fraction derived from a single exponential fit (— — —) were 8.0×10^{-9} cm^2/s and 77%, respectively.

ATP to dissociate SNARE complexes. Our complexes remained stable following this treatment because Mg^{2+} was chelated with EDTA. However, when at 52 min EDTA was replaced with Mg^{2+} and all other ingredients were kept the same, GFP-VAMP dissociated from the SNARE complexes as detected by a loss of fluorescence intensity from the surface. Dissociation continued for ~40 min. A total of ~50–60% of the SNARE complexes dissociated in this reaction. Adding another equal aliquot of the dissociation solution did not result in any further loss of fluorescence from the membrane surface (data not shown). This demonstrates that maximally ~60% of all t-SNARE complexes can be dissociated by NSF/α-SNAP in our system, which is consistent with analogous results in a reconstituted vesicle system (T. Melia, Memorial Sloan-Kettering Cancer Center, personal communication). The reason the remaining 45% appear to form a super-tight complex that cannot be dissociated by NSF, α-SNAP, and ATP when reconstituted into vesicles or in planar supported bilayers is not presently known. Addition of Mg^{2+}-ATP to GFP-VAMP/t-SNARE complexes in supported bilayers without NSF/α-SNAP did not cause dissociation of the complex (data not shown). In a separate set of control experiments, we attempted to cleave the specifically bound GFP-VAMP with BoNT D. Resistance to cleavage by BoNT D is the hallmark of SNARE complex formation (Hayashi et al., 1994). No fluorescence was released by treatment of the bilayers with BoNT D (data not shown) indicating that 100% of the t-SNARE/v-SNARE complex that was formed was part of the canonical 4-helix SNARE complex. These experiments were carried out at room temperature and 37°C. The results were the same at both temperatures.

Phosphatidylserine restricts the lateral diffusion of t-SNAREs

Cell membranes contain ~15% of the negatively charged lipid phosphatidylserine in their cytoplasmic leaflets, which topologically correspond to the outer leaflets in our model system. To approach a more physiological lipid environment, we included DOPS in the outer leaflets of the PEG-supported bilayer and studied its effects on the lateral mobility of t-SNAREs and lipids in the reconstituted membranes. When DOPS was included at increasing mole percentages (X) into a bilayer consisting of DOPC:DPS (97:3)/POPC:DOPS(100-X:X), the mobile fractions of both the NBD-eggPE lipid probe and Alexa-t-SNARE decreased (Fig. 6). At 15 mol % DOPS, i.e., the highest concentration that was tested, the mobile fractions were reduced to ~50% of what they were in the absence of DOPS. The diffusion coefficients were also slightly decreased (see legend to Fig. 6), but this effect is small on the scale of typical lateral diffusion coefficients, which can change by at least two orders of magnitude in biological membranes (see Saxton and Jacobson, 1997, for a recent review). However, the reduction in mobile fractions is significant and indicates that some parts of the membrane become immobilized by DOPS. This is unlikely due to electrostatic interactions with the quartz support because we observe similar results at pH 5 and pH 7.4, i.e., below and above the pK_a of free silanol groups on the surface of silicates (Burns et al., 1995). PEG has no charged groups that could participate in

TABLE 1 Lateral mobility of lipids and t-SNAREs in PEG and quartz-supported lipid bilayers

	Label	L:P ratio	*n*	Diffusion coefficient ($\times 10^{-9}$ cm^2/s)	Mobile fraction (%)
PEG-supported*					
	NBD-eggPE	∞	7	10.0 ± 1.0	92 ± 7
		1000:1	5	6.5 ± 0.5	88 ± 2
		400:1	5	6.0 ± 1.5	79 ± 2
	Alexa t-SNARE	1000:1	7	6.5 ± 0.5	57 ± 2
		500:1	5	7.5 ± 1.0	78 ± 3
		400:1	5	5.0 ± 1.0	44 ± 7
Quartz-supported†					
	NBD-eggPE	∞‡	5	13.0 ± 1.0	85 ± 1
		1000:1	5	14.5 ± 2.5	79 ± 5
		400:1	5	11.0 ± 4.0	75 ± 3
	Alexa t-SNARE	1000:1	7	9.5 ± 1.5	68 ± 3
		500:1	5	9.0 ± 1.0	83 ± 2
		400:1	5	8.0 ± 1.0	62 ± 4

n, number of experiments
*The bilayer consisted of DOPC:DPS (97:3) in the inner leaflet and POPC in the outer leaflet.
†The bilayer consisted of POPC in both leaflets.
‡Data from Wagner and Tamm (2000).

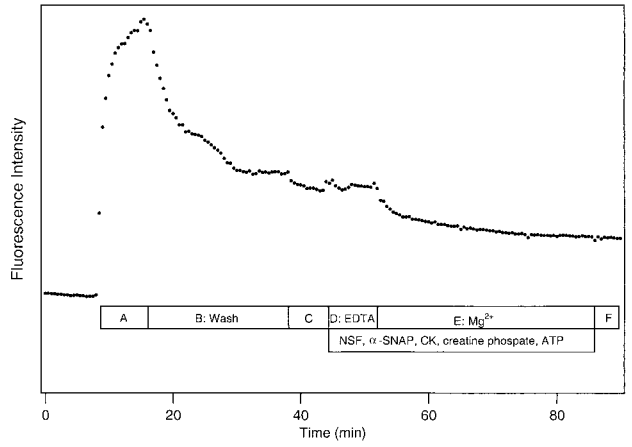

FIGURE 5 Binding and dissociation of GFP-VAMP with reconstituted t-SNARE bilayers and detected via TIRFM. A PEG-supported POPC bilayer containing t-SNAREs at a lipid:protein ratio of 400:1 was treated with 0.2 mg/ml GFP-VAMP in RB (*A*); RB (*B*); temperature raise from room temperature to 37°C (*C*); NSF, α-SNAP, VAMPh, creatine kinase, creatine phosphate, and EDTA (*D*); and NSF, α-SNAP, VAMPh, creatine kinase, creatine phosphate, and Mg^{2+} (*E*); and RB (*F*). In six different experiments, 50–60% of the specifically bound GFP-VAMP is typically dissociated by NSF/α-SNAP and Mg^{2+}-ATP in phase E.

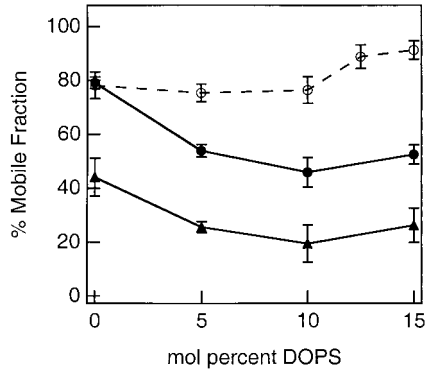

FIGURE 6 Mobile fractions of lipid and t-SNAREs in a PEG-supported bilayer as a function of increasing concentrations of phosphatidylserine. Unlabeled or Alexa-488-labeled syntaxin1A/SNAP25 were reconstituted into supported bilayers containing increasing concentrations of DOPS at a lipid:protein ratio of 400:1. ○, 2 mol % NBD-eggPE in the outer monolayer of a pure POPC lipid bilayer directly supported on quartz in the absence of protein; ●, 2 mol % NBD-eggPE in the outer monolayer of supported bilayers consisting of DOPC:DPS(97:3)/POPC:DOPS(100-X:X) containing unlabeled syntaxin1A/SNAP25. The diffusion coefficient of NBD-eggPE decreases to $(4.0 \pm 0.5) \times 10^{-9}$ cm^2/s at 15 mol % DOPS). ▲, Alexa-labeled syntaxin1A/SNAP25 reconstituted into a supported bilayer consisting of DOPC:DPS(97:3.)/POPC:DOPS(100-X:X). The bars represent standard errors from 5–10 FRAP experiments of the same bilayer. The diffusion coefficient of Alexa-labeled t-SNARE remains approximately unchanged at $(5.5 \pm 4.0) \times 10^{-9}$ cm^2/s at 15 mol % DOPS.

electrostatic interactions. The speckled appearance of the fluorescence distribution in bilayers that contained DOPS up to 15 mol % was similar to that in t-SNARE bilayers that were formed from DOPC and POPC only (Fig. 2). A few brighter spots were also seen when the t-SNARE/POPC/DOPS bilayers were labeled with NBD-eggPE (Fig. 2). When NBD-PS instead of NBD-eggPE was used as a fluorescent lipid probe, very similar images were obtained (data not shown). However, the few bright spots cannot account for the entire immobile membrane fractions. Therefore, if these fractions represent lipid domains, most of the corresponding domains must be smaller than ~300 nm in diameter or the contrast and partitioning of the probes is insufficient to visualize such domains. The lateral diffusion coefficient and the mobile fraction of NBD-PS were also similar to those of NBD-eggPE in otherwise identical bilayers. For example, the mobile fraction of NBD-PS in a t-SNARE-containing bilayer was 52 ± 11% at 15 mol % DOPS compared with

57 ± 2% of NBD-eggPE in an otherwise identical bilayer (Table 2). Therefore, selective interactions between either of these lipid probes (both are negatively charged) and t-SNAREs do not seem to exist.

PIP_2 is more effective in restricting t-SNARE diffusion than phosphatidylserine

PIP_2 is a lipid of the cytoplasmic leaflet of cell membranes that is important in many cell signaling events including some that lead to membrane fusion and secretion (Martin, 1997). PIP_2 bears three negative charges on its polar headgroup. We wanted to know whether PIP_2 interacted with t-SNAREs in the PEG-supported bilayers in a similar way as did DOPS. Therefore, we measured the lateral diffusion of Alexa-labeled t-SNAREs and lipids in bilayers consisting of DOPC:DPS (97:3)/POPC:PIP_2(100-X:X) with X ranging from 0 to 5 mol %. We again observed a large reduction in mobile fractions of the lipids and t-SNAREs in these bilayers (Fig. 7), but the lateral diffusion coefficients decreased only marginally when PIP_2 was included (see Fig. 7 legend). The reduction in mobile fraction occurred at lower concentrations of PIP_2 than DOPS, even if plotted at equivalent charge densities (i.e., 3 DOPS are equivalent to 1 PIP_2). In addition, the interaction of PIP_2 with t-SNAREs led to larger immobilized membrane fractions than the interaction with DOPS. As with DOPS we observed some, but not major lateral inhomogeneities of the fluorescence distribution when these bilayers were labeled with NBD-eggPE or Alexa 488 (Fig. 2). The mobile fraction of NBD-PIP_2 was low (20–30%) in PEG-supported bilayers irrespective of the presence of t-SNAREs (Table 3). The reason for the low lateral mobility of PIP_2 in pure lipid bilayers is not clear at the present time and requires further investigation. To our knowledge, the lateral diffusion of PIP_2 has not been measured before in model systems or cell membranes. It is interesting that the mobile fraction of the t-SNAREs in the PIP_2-containing membranes is as low as that of PIP_2 itself (compare Fig. 7 and Table 3), which raises the possibility that the t-SNAREs become sequestered into partially immobilized PIP_2 membrane domains.

TABLE 2 Effects of DOPS on the lateral mobility of lipid in SPB with and without t-SNARE complex PEG-supported bilayer

		Lipid only		Syntaxin1A/SNAP25	
Diffusing probe	Total DOPS (mol %)	D ($\times 10^{-9}$ cm^2/s)	MF (%)	D ($\times 10^{-9}$ cm^2/s)	MF (%)
	0	12.0 ± 1.5	90 ± 3	11.0 ± 0.5	75 ± 3
2% NBD-eggPE	5	5.0 ± 0.5	91 ± 5	8.5 ± 2.5	55 ± 6
	15	4.0 ± 0.5	91 ± 3	3.0 ± 0.5	57 ± 2
1% NBD-PS	5	8.0 ± 1.5	90 ± 4	4.0 ± 0.5	66 ± 2
	15	8.5 ± 1.0	94 ± 3	3.0 ± 1.5	52 ± 11

D, lateral diffusion coefficient; MF, mobile fraction.

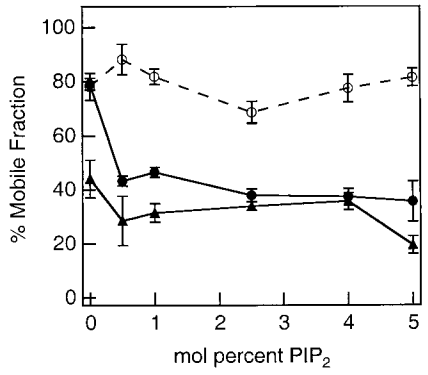

FIGURE 7 Mobile fractions of lipid and t-SNAREs in a PEG-supported bilayer as a function of increasing concentrations of PIP_2. Unlabeled or Alexa-488-labeled syntaxin1A/SNAP25 were reconstituted into supported bilayers containing increasing concentrations of PIP_2 at a lipid:protein ratio of 400:1. ○, 2 mol % NBD-eggPE in the outer monolayer of a pure POPC lipid bilayer directly supported on quartz in the absence of protein; ●, 2 mol % NBD-eggPE in the outer monolayer of supported bilayers consisting of DOPC:DPS(97:3)/POPC:PIP_2(100-X:X) containing unlabeled syntaxin1A/SNAP25. The diffusion coefficient of NBD-eggPE decreases to (2.0 ± 1.0) × 10^{-9} cm^2/s at 5 mol % PIP_2. ▲, Alexa-labeled syntaxin1A/SNAP25 reconstituted into a supported bilayer consisting of DOPC:DPS(97:3)/POPC:PIP_2(100-X:X). The bars represent standard errors from 5–10 FRAP experiments of the same bilayer. The diffusion coefficient of the Alexa-labeled t-SNARE remains approximately unchanged at (5.5 ± 3.5) × 10^{-9} cm^2/s at 5 mol % PIP_2.

TABLE 3 Effects of PIP_2 on the lateral mobility of lipid in SPB with and without t-SNARE complex on PEG-supported bilayer

		Lipid only		Syntaxin1A/SNAP25	
Diffusing probe	Total PIP_2 (mol %)	D ($\times 10^{-9}$ cm^2/s)	MF (%)	D ($\times 10^{-9}$ cm^2/s)	MF (%)
	0	12.0 ± 1.5	90 ± 3	11.0 ± 0.5	75 ± 3
2% NBD-eggPE	1	5.5 ± 0.5	82 ± 3	5.0 ± 1.0	55 ± 3
	5	6.0 ± 0.5	82 ± 3	2.5 ± 0.5	46 ± 4
1% NBD-PIP_2	1	12.0 ± 2.0	21 ± 2	2.0 ± 0.5	26 ± 5
	5	8.5 ± 1.5	23 ± 3	1.5 ± 0.5	26 ± 5

D, lateral diffusion coefficient; MF, mobile fraction.

To further investigate the specificity of PIP_2- versus DOPS-t-SNARE interactions, we systematically increased the protein:lipid ratio in the supported bilayers at a constant level of included negatively charged lipids, i.e., 15 mol % DOPS or 5 mol % PIP_2, respectively (Fig. 8), and 2 mol % NBD-eggPE was used as a probe in these lateral diffusion experiments. The results show that increasing concentrations of t-SNAREs progressively immobilize the membrane lipids if either of the negatively charged lipids is included in the bilayer. Almost no immobilization is observed as a function of protein concentration in uncharged DOPC:DPS (97:3)/POPC bilayers (open circles in Fig. 8). When compared at equal protein concentrations and lipid charge densities in the bilayer, PIP_2 is again more effective in restrict-

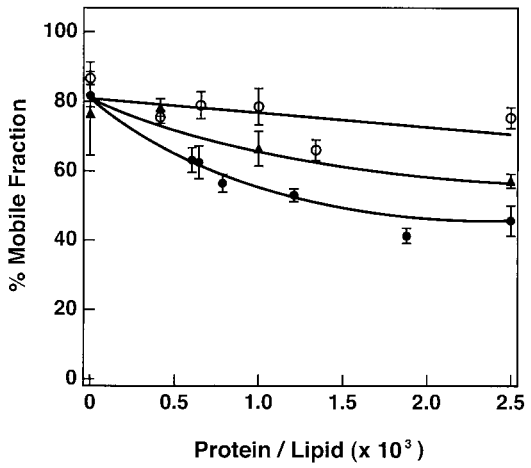

FIGURE 8 Fraction of mobile lipids in pure POPC and in DOPS and PIP_2-containing quartz-supported bilayers as a function of t-SNARE concentration in the bilayer. Unlabeled syntaxin1A/SNAP25 was reconstituted into supported POPC bilayers on quartz containing no charged lipid (POPC only, ○), 15 mol % DOPS (▲), or 5 mol % PIP_2 (●) in the outer monolayer, respectively, at increasing protein:lipid ratios. The diffusion coefficient of NBD-eggPE remained high at $(11.0 \pm 0.5) \times 10^{-9}$ cm^2/s at the highest protein concentration in pure POPC. The diffusion coefficient of NBD-eggPE decreased to $(3.0 \pm 0.5) \times 10^{-9}$ cm^2/s at 15 mol % DOPS and to $(2.5 \pm 0.5) \times 10^{-9}$ cm^2/s at 5 mol % PIP_2. The bars represent standard errors from 5–10 experiments of the same bilayer.

ing NBD-eggPE diffusion than is DOPS (closed circles versus triangles in Fig. 8). Therefore, the t-SNAREs appear to interact with PIP_2 more strongly than with DOPS. These interactions lead to partially immobilized membrane domains that restrict the lateral diffusion of the general lipid probe NBD-eggPE and, to a greater extent, the specific probe NBD-PIP_2. Syntaxin1A contains a highly basic sequence directly adjacent to the transmembrane domain (Bennett et al., 1992), which could be a candidate region for interactions with acidic lipids and particularly PIP_2.

CONCLUSIONS

In this work, we have been able to functionally reconstitute t-SNAREs into tethered polymer-supported lipid bilayers. The t-SNAREs were laterally mobile and specifically bound soluble v-SNAREs. Reconstituted SNARE complexes in supported membranes could be dissociated with NSF/α-SNAP and Mg^{2+}-ATP, but not in the absence of either one of these components. Our success with the reconstitution of SNARE function in supported bilayers now sets the stage for future biophysical experiments on the docking of v-SNARE vesicles, the role of SNAREs in membrane fusion, and structural studies on SNARE complexes in the contact region between target and vesicle membranes. Beyond these technical developments, we have shown that t-SNAREs interact with PIP_2 in a manner that restricts the lateral mobility of these two components themselves as well as the lateral mobility of the general lipid probe NBD-eggPE. Whether PIP_2 and t-SNAREs form membrane domains similar to the cholesterol-rich lipid rafts that accumulate, among other proteins, GPI-linked and doubly acylated membrane proteins (Brown and London, 1998; Simons and Toomre, 2000) is not yet known, but will be an interesting question to pursue in future studies.

We thank Drs. James Rothman, Thomas Melia, and Thomas Weber (Memorial Sloan-Kettering Cancer Center) for the generous gift of the proteins used in this study. Members of the Tamm laboratory are thanked for many helpful discussions.

This work was supported by National Institutes of Health grant AI30557.

REFERENCES

Ames, B. N. 1966. Assays of inorganic phosphate, total phosphate and phosphatases. *Methods Enzymol.* 8:115–118.

Bennett, M. K., N. Calakos, and R. H. Scheller. 1992. Syntaxin: a synaptic protein implicated in docking of synaptic vesicles at presynaptic active zones. *Science.* 257:255–259.

Block, M. R., B. S. Glick, C. A. Wilcox, F. T. Wieland and J. E. Rothman. 1988. Purification of an *N*-eythylmaleimide-sensitive protein catalyzing vesicular transport. *Proc. Natl. Acad. Sci. U.S.A.* 85:7852–7856.

Brose, N., A. G. Petrenko, T. C. Südhof, and R. Jahn. 1992. Synaptotagmin: a calcium sensor on the synaptic vesicle surface. *Science.* 256:1021–1025.

Brown, D. A., and E. London. 1998. Functions of lipid rafts in biological membranes. *Annu. Rev. Cell Dev. Biol.* 14:111–136.

Brünger, A. T. 2000. Structural insights into the molecular mechanism of Ca^{2+}-dependent exocytosis. *Curr. Opin. Neurobiol.* 10:293–302.

Burns, N. L., J. M. Van Alstine, and J. M. Harris. 1995. Poly(ethylene gycol) grafted to quartz: analysis in terms of a site-dissociation model of electroosmotic fluid flow. *Langmuir.* 11:2768–2776.

Chao, D. S., J. C. Hay, S. Winnick, R. Prekeris, J. Klumperman, and R. H. Scheller. 1999. SNARE membrane trafficking dynamics in vivo. *J. Cell Biol.* 144:869–881.

Clary, D. O., I. C. Griff, and J. E. Rothman. 1990. SNAPs, a family of NSF attachment proteins involved in intracellular membrane fusion in animals and yeast. *Cell.* 61:709–721.

Cremer, P. S., and S. Boxer. 1999. Formation and spreading of lipid bilayers on planar glass supports. *J. Phys. Chem. B.* 103:2554–2559.

Ferro-Novick, S., and P. Novick. 1993. The role of GTP-binding proteins in transport along the exocytic pathway. *Annu. Rev. Cell Biol.* 9:575–599.

Glenn, D. E., and R. D. Burgoyne. 1996. Botulinum neurotoxin light chains inhibit both Ca^{2+}-induced and GTP-analog-induced catecholamine release from permeabilized adrenal chromaffin cells. *FEBS Lett.* 386: 137–140.

Hanson, P. I., J. E. Heuser, and R. Jahn. 1997. Neurotransmitter release: four years of SNARE complexes. *Curr. Opin. Neurobiol.* 7:319–315.

Hayashi, T., H. McMahon, S. Yamasaki, T. Binz, Y. Hata, T. C. Südhof, and H. Niemann. 1994. Synaptic vesicle membrane fusion complex: action of clostridial neurotoxins on assembly. *EMBO J.* 13:5051–5061.

Hayashi, T., S. Yamasaki, S. Nauenburg, T. Binz, and H. Niemann. 1995. Disassembly of the reconstituted synaptic vesicle membrane fusion complex in vitro. *EMBO J.* 14:2317–2325.

Hinterdorfer, P., G. Baber, and L. K. Tamm. 1994. Reconstitution of membrane fusion sites. A total internal reflection fluorescence microscopy study of influenza hemagglutinin-mediated membrane fusion. *J. Biol. Chem.* 269:20360–20368.

Jahn, R., and T. C. Südhof. 1999. Membrane fusion and exocytosis. *Annu. Rev. Biochem.* 68:863–911.

Kalb, E., J. Engel, and L. K. Tamm. 1990. Binding of proteins to specific target sites in membranes measured by total internal reflection fluorescence spectroscopy. *Biochemistry.* 29:1607–1613.

Kalb, E., S. Frey, and L. K. Tamm. 1992. Formation of supported planar bilayers by fusion of vesicles to supported phospholipid monolayers. *Biochim. Biophys. Acta.* 1103:307–316.

Martin, T. F. J. 1997. Phosphoinositides as spatial regulators of membrane traffic. *Curr. Opin. Neurobiol.* 7:331–338.

McConnell, H. M., T. H. Watts, R. M. Weis, and A. A. Brian. 1986. Supported planar membranes in studies of cell-cell recognition in the immune system. *Biochim. Biophys. Acta.* 864:95–106.

McNew, J. A., T. Weber, D. M. Engelman, T. H. Söllner, and J. E. Rothman. 1999. The length of the flexible SNAREpin juxtamembrane region is a critical determinant of SNARE-dependent fusion. *Mol. Cell.* 4:415–421.

Misura, K. M. S., R. H. Scheller, and W. I. Weis. 2000. Three-dimensional structure of the neuronal-nSec1-syntaxin 1a complex. *Nature.* 404: 355–362.

Ostermeier, C., and A. T. Brünger. 1999. Structural basis of Rab effector specificity: crystal structure of the small G protein Rab3A complexed with the effector domain of rabphilin-3A. *Cell.* 96:363–374.

Parlati, F., T. Weber, J. A. McNew, B. Westermann, T. H. Söllner, and J. E. Rothman. 1999. Rapid and efficient fusion of phospholipid vesicles by the α-helical core of a SNARE complex in the absence on an N-terminal regulatory domain. *Proc. Natl. Acad. Sci. U.S.A.* 96:12565–12570.

Poirier, M. A., W. Xiao, J. C. Macosko. C. Chan, Y-K. Shin, and M. K. Bennett. 1998. The synaptic SNARE complex is a parallel four-stranded helical bundle. *Nat. Struct. Biol.* 5:765–769.

Rothman, J. E., and F. T. Wieland. 1996. Protein sorting by transport vesicles. *Science.* 272:227–234.

Sackmann, E. 1996. Supported membranes: scientific and practical applications. *Science.* 271:43–48.

Saxton, M. J., and K. Jacobson. 1997. Single-particle tracking: applications to membrane dynamics. *Annu. Rev. Biophys. Biomol. Struct.* 26: 373–399.

Simons, K., and D. Toomre. 2000. Lipid rafts and signal transduction. *Nat. Rev. Mol. Cell Biol.* 1:31–39.

Söllner, T. H., M. K. Bennett, S. W. Whiteheart, R. H. Scheller, and J. E. Rothman. 1993a. A protein assembly-disassembly pathway in vitro that may correspond to sequential steps of synaptic vesicle docking, activation, and fusion. *Cell.* 75:409–418.

Söllner, T. H., S. W. Whiteheart, M. Brunner, H. Erdjument-Bromage, S. Geromanos, P. Tempst, and J. E. Rothman. 1993b. SNAP receptors implicated in vesicle targeting and fusion. *Nature.* 362:318–324.

Südhof, T. C., M. Baumert, M. S. Perin, and R. Jahn. 1989. A synaptic vesicle membrane protein is conserved from mammals to *Drosophila*. *Neuron.* 2:1475–1481.

Sutton, R. B., J. A. Ernst, and A. T. Brünger. 1999. Crystal structure of the cytosolic C2A-C2B domains of synaptotagmin. III. Implications for Ca^{2+}-independent SNARE complex formation. *J. Cell Biol.* 147: 589–598.

Sutton, R. B., D. Fasshauer, R. Jahn, and A. T. Brünger. 1998. Crystal structure of a SNARE complex involved in synaptic exocytosis at 2.4 Å resolution. *Nature.* 395:347–353.

Tamm, L. K. 1988. Lateral diffusion and fluorescence microscope studies on a monoclonal antibody specifically bound to supported phospholipid bilayers. *Biochemistry.* 27:1450–1457.

Tamm, L. K. 1993. Total internal reflectance fluorescence microscopy. *In* Optical Microscopy: Emerging Methods and Applications. Academic Press, New York. 295–337.

Tamm, L. K., and H. M. McConnell. 1985. Supported phospholipid bilayers. *Biophys. J.* 47:105–113.

Toomre, D., J. A. Steyer, P. Keller, W. Almers, and K. Simons. 2000. Fusion of constitutive membrane traffic with the cell surface observed by evanescent wave microscopy. *J. Cell Biol.* 149:33–40.

Ungermann, C., B. J. Nichols, H. R. B. Pelham, and W. Wickner. 1998. A vacuolar v-t SNARE complex, the predominant forms in vivo and on isolated vacuoles, is disassembled and activated for docking and fusion. *J. Cell Biol.* 140:61–69.

Wagner, M. L., and L. K. Tamm. 2000. Tethered polymer-supported planar lipid bilayers for reconstitution of integral membrane proteins: silane-polyethyleneglycol-lipid as a cushion and covalent linker. *Biophys. J.* 79:1400–1414.

Weber, T., B. V. Zemelman, J. A. McNew, B. Westermann, M. Gmachi, F. Parlati, T. H. Söllner, and J. E. Rothman. 1998. SNAREpins: minimal machinery for membrane fusion. *Cell.* 92:759–772.

Whiteheart, S. W., K. Rossnagel, S. H. Buhrow, M. Brunner, R. Jaenicke, and J. E. Rothman. 1994. *N*-ethylmaleimide-sensitive fusion protein: a trimeric ATPase whose hydrolysis of ATP is required for membrane fusion. *J. Cell Biol.* 126:945–954.

Zenisek, D., J. A. Steyer, and W. Almers. 2000. Transport, capture and exocytosis of single synaptic vesicles at active zones. *Nature.* 406: 849–854.